

Mössbauer studies of α'' -Fe₁₆N₂ and α' -Fe₈N films

Z. W. LI, A. H. MORRISH

Department of Physics, University of Manitoba, Winnipeg, Canada R3T 2N2
E-mail: amorrsh@cc.umanitoba.ca

C. ORTIZ

IBM Research Division, Almaden Research Center, San Jose, California 95120, USA

Conversion-electron Mössbauer spectra of epitaxial α'' -Fe₁₆N₂ and α' -Fe₈N films have been studied and their differences are discussed in detail. The Mössbauer spectrum of α'' -Fe₁₆N₂ can be decomposed into three subspectra, which correspond to the 4*d*, 8*h* and 4*c* sites. The Mössbauer spectrum of α' -Fe₈N can be fitted using four spectra based on a nitrogen-atom-random-distribution model. The average hyperfine field is larger (3%) for α'' -Fe₁₆N₂ than for α' -Fe₈N, which is approximately consistent with a 4.1% enhancement of the magnetic moments for α'' -Fe₁₆N₂. The iron moments tend to locate in the film plane for α'' -Fe₁₆N₂ and to arrange perpendicularly to the film plane for α' -Fe₈N.

© 2001 Kluwer Academic Publishers

1. Introduction

Since Kim and Takahashi (1972) [1] and Komuro *et al.* (1990) [2] proposed that the α'' -Fe₁₆N₂ phase has a saturation magnetization, σ_s , superior to that of α -Fe (216 emu/g), this compound has attracted much attention. However, the reported values of σ_s for α'' -Fe₁₆N₂ vary considerably, from 226 emu/g [3] to 310 emu/g [4]. Mössbauer spectra of α'' -Fe₁₆N₂ have also been extensively studied and significantly different results were reported. The Sugita group [5, 6] found only one type of iron atom with a hyperfine field of about 40.0 T. However, most Mössbauer measurements [7–14] for α'' -Fe₁₆N₂ gave three hyperfine fields corresponding to three different iron sites, as expected for the crystal structure. Besides, the values obtained for the hyperfine fields have great differences, from 37.0 T to over 41.8 T for the 4*d* site. Most researchers focus on the α'' -Fe₁₆N₂ film. A few [8] have reported on Mössbauer studies of α' -Fe₈N, especially on the difference between the Mössbauer spectra of α'' -Fe₁₆N₂ and α' -Fe₈N. The current status of iron-nitride systems has been reviewed recently by Coey and Smith [15]. In this paper we report Mössbauer studies of epitaxial α' -Fe₈N and α'' -Fe₁₆N₂ films prepared using the same technology and under the same conditions.

2. Experimental

The template used was grown by dc sputtering an iron film with the thickness of 3 nm followed by rf sputtering a buffer of silver with a thickness of 100 nm onto the cleaved MgO (001) substrate held at 100°C. Then, the template was cooled to room temperature and the Fe/N deposition was carried out in a mixture of argon and nitrogen gases. The entrances of the gases

were controlled independently by the flow meters; the controls were set for a stable flow of 46 and 4 sccm (standard cubic centimeter per minute). A deposition rate of 0.02 nm/s was used to obtain the 11.2 at.% N₂ composition. As deposited, disordered α' -Fe₈N was formed. The thickness is about 100 nm. The film was annealed in vacuum (at least 10⁻⁶ Torr) at 150°C for 2 h to produce α'' -Fe₁₆N₂. Further sample preparation details were reported in Ref. [16]

X-ray diffraction was carried out using an x-ray diffractometer with Cu K α . The patterns for α' -Fe₈N and α'' -Fe₁₆N₂ are shown in Fig. 1. The line at $2\theta = 28.5^\circ$ is characteristic for the (002) reflection of the ordered α'' -Fe₁₆N₂. By analyzing the areas of the (002) and (004) ($2\theta = 58.6^\circ$) lines in Fig. 1a, the ratio of the α'' and α' phases in the α'' -Fe₁₆N₂ film is 85 : 15.

The magnetizations were measured with a vibrating sample magnetometer (VSM) in an external magnetic field of up to 1.0 T applied parallel to the sample plane. Magnetic saturation is reached in a magnetic field between 0.6 and 0.8 T. The contribution of the 3.0 nm iron template was subtracted by the following procedure. First the Fe was deposited in two different thick layers, for example 100 and 200 nm, whose thickness and magnetic moment can be measured precisely. Obviously, the time of deposition of the first layer is half that of the second one. By linear extrapolation the time needed to deposit the final Fe thin layer is then determined. Then the magnetization of the substrate and also the substrate with the 200 nm Fe layer were determined and the difference recorded. Finally, the magnetization of the thin Fe layer whose thickness is known from the extrapolation procedure is obtained.

In order to determine the thickness of the sputtered iron-nitride films, calibrations were made by first

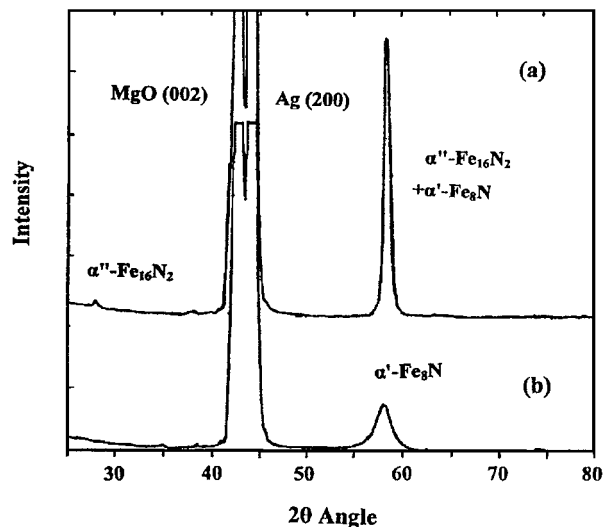


Figure 1 X-ray diffraction patterns for (a) α'' -Fe₁₆N₂ and (b) α' -Fe₈N.

depositing very thick films and then reducing the sputtering time to obtain the much thinner films. A typical magnetization curve is shown by Ortiz *et al.* [16]. The saturation magnetization is believed to be correct within 2–3%. For α' -Fe₈N the magnetization found is 240(6) emu/g and for α'' -Fe₁₆N₂ the value is 250 (6) emu/g.

Mössbauer spectra at room temperature were obtained from CEMS (conversion electron Mössbauer spectroscopy). The detector used was a gas flow design and about 2 million counts per channel were collected. The source was ⁵⁷Co in a Rh matrix. The calibration was made using an α -Fe spectrum.

3. Results and discussion

Mössbauer spectra and the computer fitted curves for α'' -Fe₁₆N₂ and α' -Fe₈N are shown in Fig. 2. The quality of these spectra is as good or better than those reported previously in the literature for iron-nitride films. The fitted hyperfine parameters are listed in Table I. The Mössbauer spectrum of α'' -Fe₁₆N₂ film was fitted using five subspectra. Three of them correspond to the three Fe sites, the 4*d*, 8*h* and 4*c* sites. The fourth subspectrum with a hyperfine field of 33.5 T, quadrupole splitting of 0.01 mm/s and isomer shift of

TABLE I Mössbauer parameters of α'' -Fe₁₆N₂ and α' -Fe₈N at room temperature. Here, δ is the isomer shift with respect to α -Fe, ϵ is the quadrupole splitting, B_{hf} is the hyperfine field, b is the area ratio of the 2nd plus 5th to the 3rd plus 4th and S is the relative area

Number		δ (mm/s)	ϵ (mm/s)	B_{hf} (T)	b	S (%)
α'' -Fe ₁₆ N ₂						
Fe 1	4 <i>d</i>	0.03(2)	-0.04(2)	37.2(3)	2.34(20)	22(2)
Fe 2	8 <i>h</i>	0.09	0.09	31.5	2.34	43(6)
Fe 3	4 <i>c</i>	0.06	-0.11	28.5	2.34	21(3)
Fe 4	α -Fe	0.07	0.01	33.5	0.88	10(2)
Fe 5		0.08	0.55			5(1)
α' -Fe ₈ N						
Fe 1	P(0)	0.03(2)	0.04(2)	37.4(3)	0.98(20)	17(2)
Fe 2	P(1)	0.11	0.02	31.8	0.98	32(2)
Fe 3	P(2)	0.14	-0.02	29.2	0.98	26(2)
Fe 4	P(3)	0.16	0.07	25.0	0.98	10(2)
Fe 5	α -Fe	0.04	0.00	33.8	1.00	7(1)
Fe 6		0.13	0.92			8(1)

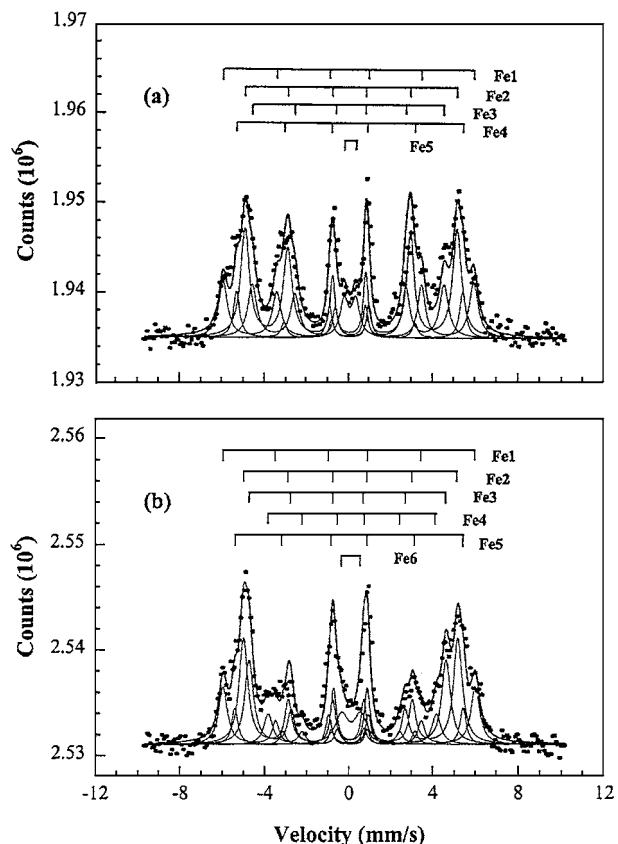


Figure 2 Mössbauer spectra and their fitted curves for (a) α'' -Fe₁₆N₂ and (b) α' -Fe₈N.

0.07 mm/s has almost the same hyperfine parameters as α -Fe. Therefore, it is ascribed to an α -Fe part remaining in the nitrified film. The fraction of α -Fe is roughly estimated to be 10% based on the relative area for the Mössbauer subspectrum. The fifth subspectrum is a doublet with quadrupole splitting of 0.55 mm/s and isomer shift of 0.08 mm/s. Perhaps, it has its origin in paramagnetism or superparamagnetism at the boundary between the Fe and Ag layers. The relative area of the doublet is about 5%.

The Mössbauer spectrum of the α' -Fe₈N film was fitted using six subspectra. Four of them were assigned to the α' -Fe₈N. An α -Fe and a doublet (subspectra 5 and 6 in Fig. 2b) are also observed.

3.1. α'' -Fe₁₆N₂

From the structural viewpoint, α'' -Fe₁₆N₂ has a tetragonal structure with space group I4/mmm. Iron atoms occupy three sites designated as 4*d*, 8*h* and 4*c*, as shown in Fig. 3a. The site occupation ratio is 1 : 2 : 1, with four iron atoms on the 4*d* site, eight on the 8*h* and four on the 4*c* sites. On the other hand, the relative areas are 22(2), 43(6) and 21(3)% for subspectra 1, 2 and 3, respectively, very close to a ratio of 1 : 2 : 1. Based on the subspectral areas, it is easy to distinguish the 8*h* site from the 4*d* and 4*c* sites.

The hyperfine fields for α'' -Fe₁₆N₂ are greatly different from that of 33.1 T for α -Fe; one is much larger and the others are smaller. The differences are related to the different locations for the nitrogen atoms around each iron site. It is known that the interstitial nitrogen

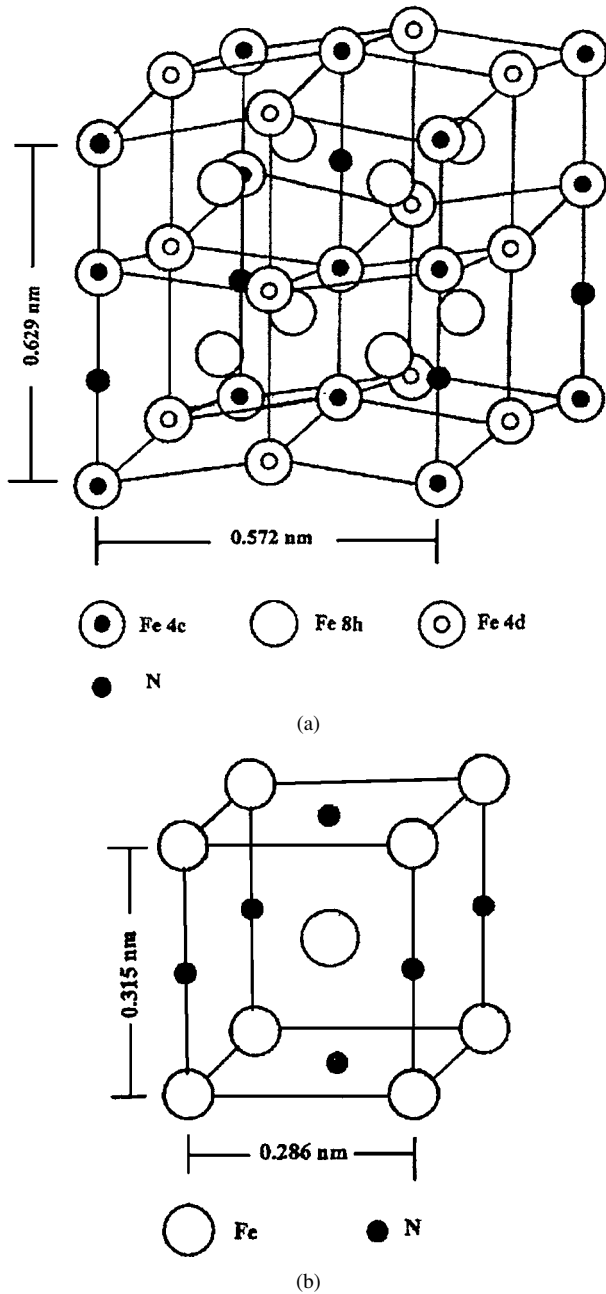


Figure 3 Crystal structure for (a) $\alpha''\text{-Fe}_{16}\text{N}_2$ and (b) $\alpha'\text{-Fe}_8\text{N}$.

atoms have two opposite influences on the hyperfine fields. First, the interstitial nitrogen atoms expand the lattice. The magnitude of the hyperfine field is related to the interatomic distances between the iron atoms. The larger interatomic distance can lead to an increase in hyperfine field. Nakajima *et al.* [10] also indicated that if the volume expansion increases the state density of the 4s electrons, the magnetic moment of an iron atom may possibly exceed $3 \mu_B$. Second, the adjacent nitrogen atoms lead to a decrease in the hyperfine field because of the hybridization between the iron and its adjacent nitrogen atoms for iron-nitrogen compounds [17]. For example, Fe_4N has significantly different hyperfine fields, as high as 34.5 T for the site with no adjacent nitrogen atoms but only 21.5 T for the site with two adjacent nitrogen atoms [18]. Based on the above factors, we assign the maximum hyperfine field of 37.2 T to the 4d site because this site has no adjacent nitrogen atoms and, respectively, the fields of 31.5 and 28.5 T to the 8h

and 4c sites for these two sites have one nitrogen atom as their neighbor.

3.2. $\alpha'\text{-Fe}_8\text{N}$

Both $\alpha'\text{-Fe}_8\text{N}$ and $\alpha''\text{-Fe}_{16}\text{N}_2$ have the tetragonal structure. However, the nitrogen atoms orderly occupy the interstitial sites for $\alpha''\text{-Fe}_{16}\text{N}_2$ but are randomly distributed in the interstitial sites for $\alpha'\text{-Fe}_8\text{N}$. The Mössbauer spectrum of $\alpha'\text{-Fe}_8\text{N}$, as shown in Fig. 2b has similarities to the spectrum of $\alpha''\text{-Fe}_{16}\text{N}_2$. However, there exist three significant differences. First, an extra spectral line at a velocity of about -4 mm/s is observed for $\alpha'\text{-Fe}_8\text{N}$. Second, the relative area of subspectra 2 is close to that of subspectrum 3 for $\alpha'\text{-Fe}_8\text{N}$ but the area of subspectrum 2 is about twice the area of subspectrum 3 for $\alpha''\text{-Fe}_{16}\text{N}_2$. Finally, the total area ratios between the 2nd plus 5th lines and the 3rd plus 4th lines are 2.34 for $\alpha''\text{-Fe}_{16}\text{N}_2$ and only 0.98 for $\alpha'\text{-Fe}_8\text{N}$. The differences (1) and (2) imply a different arrangement of nitrogen atoms in $\alpha'\text{-Fe}_8\text{N}$ and $\alpha''\text{-Fe}_{16}\text{N}_2$ films.

Based on the binomial distribution model, the probabilities of finding m adjacent nitrogen atoms for the iron sites are given by

$$P(m) = \frac{n!}{m!(n-m)!} c^m (1-c)^{n-m} \quad (1)$$

where n is the number of adjacent interstitial sites around the iron site, and c is the relative nitrogen concentration to the interstitial sites and can be expressed as

$$c = \frac{c'}{z(1-c')} \quad (2)$$

where $z = 1$ is the ratio between the numbers of the interstitial sites to the iron sites in a unit cell and $c' = 1/9$ is the nitrogen concentration in the film.

The structure of $\alpha'\text{-Fe}_8\text{N}$ is shown in Fig. 3b. Here, the first three neighbouring shells of interstitial sites are considered; around an iron atom there are fourteen adjacent nitrogen sites ($n = 14$; two nearest neighbours, four second neighbours and eight third neighbours). The probabilities calculated from Equations 2 and 3, as shown in TABLE II, are approximately consistent with the relative areas of the Mössbauer subspectra. This indicates that there is a random distribution of nitrogen atoms in $\alpha'\text{-Fe}_8\text{N}$.

The average hyperfine fields over the three or four subspectra are 32.2 and 31.3 T for $\alpha''\text{-Fe}_{16}\text{N}_2$ and $\alpha'\text{-Fe}_8\text{N}$, respectively. As compared to $\alpha'\text{-Fe}_8\text{N}$, the

TABLE II The probabilities, $P(m)$, calculated based on the random model and Mössbauer spectral areas for $\alpha'\text{-Fe}_8\text{N}$. P^* and S^* are normalized values of P and S , respectively, based on the total

m	$P(m)$	$P^*(m)$	$S(\%)$	S^*
0	0.15	0.17	17	0.20
1	0.31	0.34	32	0.38
2	0.29	0.31	26	0.30
3	0.16	0.18	10	0.12
Total	0.91	1.00	85	1.00

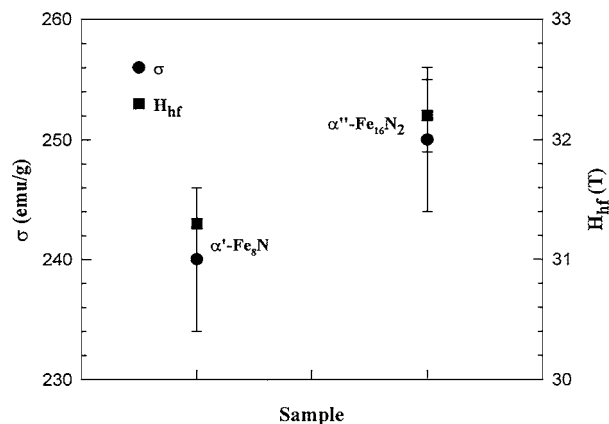


Figure 4 Magnetizations and average hyperfine fields for $\alpha''\text{-Fe}_{16}\text{N}_2$ and $\alpha'\text{-Fe}_8\text{N}$.

average hyperfine field of $\alpha''\text{-Fe}_{16}\text{N}_2$ has a 3.0% enhancement. The magnetic moments measured by a VSM are 250(6) and 240(6) emu/g for $\alpha''\text{-Fe}_{16}\text{N}_2$ and $\alpha'\text{-Fe}_8\text{N}$, respectively; thus the moment of $\alpha''\text{-Fe}_{16}\text{N}_2$ is increased by about 4.1%. The results obtained from Mössbauer spectra and the magnetization measurements are very close, as shown in Fig. 4. From Table I, we find that for $\alpha'\text{-Fe}_8\text{N}$ the hyperfine fields of subspectra 1, 2 and 3 are close to or even slightly larger than those for $\alpha''\text{-Fe}_{16}\text{N}_2$. However, an extra subspectrum with a small hyperfine field of 25.0 T exists in $\alpha'\text{-Fe}_8\text{N}$ and may be responsible for the slightly lower average hyperfine field.

The direction of the iron moments can be obtained from the Mössbauer spectra. The area ratio between the 2nd plus 5th, $A_{2,5}$, and the 3rd plus 4th, $A_{3,4}$, lines gives an average direction, $\langle\theta\rangle$, for the iron moment distributions relative to the normal of the film plane, based on the equation

$$\langle\theta\rangle = \cos^{-1} \sqrt{\frac{4 - A_{2,5}/A_{3,4}}{4 + A_{2,5}/A_{3,4}}} \quad (3)$$

The fitted ratios are 0.98 and 2.34 for $\alpha'\text{-Fe}_8\text{N}$ and $\alpha''\text{-Fe}_{16}\text{N}_2$, respectively. The corresponding angles, $\langle\theta\rangle$, are 38.8° and 59.2° . This implies that the iron moments tend to arrange perpendicularly to the film for $\alpha'\text{-Fe}_8\text{N}$ and to locate in the film plane for $\alpha''\text{-Fe}_{16}\text{N}_2$.

4. Conclusions

1. The Mössbauer spectrum of $\alpha''\text{-Fe}_{16}\text{N}_2$ can be decomposed into three subspectra, which correspond to the 4d, 8h and 4c sites. The Mössbauer spectrum of $\alpha'\text{-Fe}_8\text{N}$ can be fitted using four subspectra based on a nitrogen-atom-random-distribution model.

2. Mössbauer spectra show that the average hyperfine field is larger by 3.0% for $\alpha''\text{-Fe}_{16}\text{N}_2$ as compared

to that for $\alpha'\text{-Fe}_8\text{N}$, which is consistent with a 4.1% enhancement of the saturation magnetization for $\alpha''\text{-Fe}_{16}\text{N}_2$. On a micro-scale, the hyperfine field at each iron site has a different value because of the various local environments. The hyperfine fields of $\alpha''\text{-Fe}_{16}\text{N}_2$ are distributed from 37.2 to 28.5 T. However, the fields of $\alpha'\text{-Fe}_8\text{N}$ extend down to 25.0 T. The extra component with the small hyperfine field leads to a slightly smaller average field, i.e. a smaller magnetization, as compared to $\alpha''\text{-Fe}_{16}\text{N}_2$.

3. The iron moments tend to arrange perpendicularly to the film surface for $\alpha'\text{-Fe}_8\text{N}$ and to locate in the film plane for $\alpha''\text{-Fe}_{16}\text{N}_2$.

Acknowledgment

This research at the University of Manitoba was supported financially by the Natural Sciences and Engineering Research Council of Canada.

References

1. T. K. KIM and M. TAKAHASHI, *Appl. Phys. Lett.* **20** (1972) 492.
2. M. KOMURO, Y. KOZONO, M. HANAZONO and Y. SUGITA, *J. Appl. Phys.* **67** (1990) 5126.
3. M. TAKAHASHI, H. SHOKI, H. TAKAHASHI and M. WAKIYAMA, *IEEE Trans. Magn.* **29** (1993) 102.
4. H. TAKAHASHI, K. MITSUOKA, M. KOMURO and Y. SUGITA, *J. Appl. Phys.* **73** (1993) 6060.
5. Y. SUGITA, K. MITSUOKA, M. KOMURO, H. HOSHIYA, Y. KOZONO and M. HANAZONO, *ibid.* **70** (1991) 5977.
6. Y. SUGITA, H. TAKAHASHI, M. KOMURO, K. MITSUOKA and A. SAKUNIA, *ibid.* **76** (1994) 6637.
7. J. FOCT, *J. de Phys.* **35** (1974) C6-487.
8. T. MORIJA, Y. SUMITOMO, H. INO, F. E. FUJITA and Y. MACDA, *J. Phys. Soc. Jpn.* **35** (1973) 1378.
9. K. NAKAJIMA, S. OKAMOTO and T. OKADA, *J. Appl. Phys.* **65** (1989) 4357.
10. K. NAKAJIMA, T. YAMASHITA, M. TAKATA and S. OKAMOTO, *ibid.* **70** (1991) 6033.
11. M. TAKAHASHI, H. SHOJI, H. TAKAHASHI, T. WAKIYAMA, M. KINOSHITA and W. OHTA, *IEEE Trans. Magn.* **29** (1993) 3040.
12. M. TAKAHASHI, H. SHOJI, H. TAKAHASHI, H. HASHI, T. WAKIYAMA, M. DOI and M. MATSIU, *J. Appl. Phys.* **76** (1994) 6642.
13. J. M. D. COEY, K. O'DONNELL, Q. QI, E. TOUCHAIS and K. H. JACK, *J. Phys. C: Condens. Matter* **6** (1994) L23.
14. J. M. D. COEY, *J. Appl. Phys.* **76** (1994) 6632.
15. J. M. D. COEY and P. A. I. SMITH, *J. Magn. Magn. Mat.* **200** (1999) 405.
16. C. ORTIZ, G. DUMPICH and A. H. MORRISH, *Appl. Phys. Lett.* **65** (1994) 2737.
17. Z. W. LI, X. Z. ZHOU and A. H. MORRISH, *J. Phys. C: Condens. Matter* **4** (1992) 10409.
18. G. SHIRANE, T. TAKEI and L. RUBY, *Phys. Rev.* **126** (1962) 49.

Received 16 October 2000

and accepted 10 August 2001